Article

Fluorescent Silver Nanoclusters Embedded in Hydrogel Matrix and Its Potential Use in Environmental Monitoring

Luca Burratti [1,*] , Fabio De Matteis [1,2] , Roberto Francini [1,2] , Joohyun Lim [3], Christina Scheu [4] and Paolo Prosposito [1,2]

1   Department of Industrial Engineering and INSTM, University of Rome Tor Vergata, Via del Politecnico 1, 00133 Rome, Italy; demattei@roma2.infn.it (F.D.M.); francini@roma2.infn.it (R.F.); paolo.prosposito@uniroma2.it (P.P.)
2   Center for Regenerative Medicine—CIMER, University of Rome Tor Vergata, Via Montpellier 1, 00133 Rome, Italy
3   Department of Chemistry, Kangwon National University, Chuncheon 24341, Korea; jlim@kangwon.ac.kr
4   Max-Planck-Institut für Eisenforschung GmbH, Max-Planck-Straße 1, 40237 Düsseldorf, Germany; c.scheu@mpie.de
*   Correspondence: luca.burratti@uniroma2.it

Abstract: The optical absorption and fluorescence of silver nanoclusters (AgNCs) are widely exploited in many different application fields such as sensors, bio-imaging, drug delivery, etc. In the sensor field, optical devices are highly versatile thanks to their ease of fabrication and low costs and, therefore, are optimal candidates to replace expensive apparatuses commonly used. In this study, we synthesized AgNCs in aqueous phase by photochemical synthesis using poly methacrylic acid (PMAA) as a stabilizer. Colloidal water solutions of these NCs showed a very good sensitivity to Pb(II) ions, and in order to fabricate a solid-state sensor, we introduced them in a hydrogel material formed by poly(ethylene glycol) diacrylate with a molecular weight of 700 g/mol (PEGDA$_{700}$). The systems were characterized using absorption and fluorescence spectroscopy and transmission electron microscopy (TEM). Finally, the sensitivity to Pb(II) ions has been tested with the aim to use these systems as solid-state optical sensors for water quality.

Keywords: silver nanoclusters; hydrogel matrix; Pb(II) ions detection; fluorescent spectroscopy

1. Introduction

Nanomaterials have aroused a great interest in the research field due to their chemo-physical properties that are not owned by the material itself but that appear for their reduced size. For instance, noble metal nanomaterials have attracted wide attention in past years due to their unique optical properties. Metals have free electrons in the conduction band that determine their high electrical conductivity and optical reflectivity. When the particle dimensions decrease, approaching tens of nanometers as in the case of nanoparticles (NPs), electron motion on the particles surface dominates. When an electromagnetic wave (visible light) interacts with NPs, the physical phenomena of Localized Surface Plasmon Resonance (LSPR) occur, i.e., a collective oscillation of conduction electrons upon interaction with the light. Colloidal suspensions of metal NPs display intense colors, thus, in the absorption spectra, characteristic bands appear that depend on the type of metal and on the dimension and shape [1–5]. When the NPs size decreases below 2 nm, the nanostructures are named nanoclusters (NCs), and present a different optical behavior. In this case, discrete energy levels instead of bands are present and the electronic transitions, induced by the interaction with electromagnetic wave, produce absorption and fluorescence. Consequently, NCs systems show not only characteristic bands in the absorbance spectra but also bright luminescence [6–10]. The number of atoms composing the metal nanoclusters and their shape play an important role in the absorption and emission spectra [11–13].

Metal nanoclusters can be synthesized by chemical reduction [14–16], starting from a precursor salt of the desired metal and using a reducing agent, which reduces the metal ions into metal atoms. Alternatively, especially in water synthesis, the reducing agent can be a physical one, such as strong UV radiation [17,18] or ultrasonic waves [19,20], which produce radicals from the H_2O molecules, and these radicals are responsible for the reduction of metal ions into metal atoms.

Colloidal suspensions of metal NCs can be exploited for different applications such as fluorescent labels for bioimaging [21–23], drug-delivery [24–26], catalytic applications [27–29] and environmental monitoring [30–32].

Analytical techniques with high selectivity and sensitivity are commonly employed to detect water pollutants, such as atomic absorption spectroscopy (AAS) [33], atomic emission spectroscopy (AES) [34], chromatography [35], or mass spectrometry (MS) [36], but these methods are expensive and time-consuming, mainly due to the sample preparation [37]. On the other side, simple sensor devices based on changes of the optical absorption and/or fluorescence in the presence of heavy metal ions are highly desirable for the low costs and for the ease of use based on simple and portable UV-Vis spectrometer. Colloidal solutions of fluorescent metal NCs as sensors have been widely studied and used in laboratory facilities [38–42], but rarely employed for in situ detection. The solid-state sensors have many advantages with respect to the colloidal ones in terms of handling or mechanical stability. For instance, with a solid device it would be possible to map quickly and accurately a certain area; indeed, placing in contact directly the sensor with the contaminated place, avoiding sampling procedures and thus saving time. Some papers report the encapsulation of metal-nanomaterials in solid matrices [43–48], but only few report their exploitation for heavy metal ions detection purpose [49–53]. One of the most employed polymers for the synthesis of hydrogel matrix is the poly(ethylene glycol) PEG and its derivatives, due to their very simple way to make crosslinks after UV radiation exposure [54,55]. In addition, the employment of the PEG derivatives as matrices for environmental monitoring could be strategic for the high swelling factor in water [56,57], allowing a fast diffusion of pollutant cations inside the matrix and facilitating the interaction with the sensitive moiety (NCs in our case).

In this work, we report on the synthesis of silver nanoclusters (AgNCs) stabilized by poly(methacrylic acid) (PMAA). We studied the optical properties of the AgNCs-PMAA system in a water solution and in a hybrid hydrogel matrix based on PEGDA. AgNCs-PMAA show a fluorescence peaked at 660 nm when excited with a LED source at 340 nm. The fluorescence band is independent from the excitation wavelength (within the range 340–540 nm), indicating a high monodispersion in size [58,59]. The average size of the synthesized NCs was 1.84 nm, measured by High-Resolution Transmission Electron Microscopy (HRTEM). We tested hybrid hydrogel samples in the presence of several metal ions. The sensitivity to Pb(II) ions found in liquid solution, was preserved in the solid-state device. The interaction kinetics between the Pb(II) cations and the matrix containing the fluorescent material was evaluated. The performance of the hybrid device in terms of limit of detection (LOD) and linear behavior (form 0 to 100 μM) as a function of AgNCs-PMAA content were also studied. This result represents a first step toward the fabrication of a solid-state optical sensor for water quality monitoring based on fluorescent AgNCs-PMAA.

2. Materials and Methods

2.1. Chemical Products

Silver nitrate ($AgNO_3$), poly(methacrylic acid) sodium salt solution (MW = 9400, 30% wt. in water), poly(ethylene glycol) diacrylate ($PEGDA_{700}$, Mn = 700), ethanol (>99.8%), and nitric acid HNO_3 (70%) were purchased from Sigma-Aldrich (St. Luis, Missouri, USA). The photoinitiator Irgacure 819 was purchased from Ciba Specialty Chemicals (Basel, Switzerland). All reagents were used without any further purifications. For sensing tests, the following metal precursor salts were used: copper nitrate pentahydrate [$Cu(NO_3)_2 \cdot 5H_2O$], lead nitrate [$Pb(NO_3)_2$], zinc nitrate hexahydrate [$Zn(NO_3)_2 \cdot 6H_2O$],

cadmium nitrate pentahydrate [$Cd(NO_3)_2 \cdot 5H_2O$], sodium nitrate [$NaNO_3$], nickel chloride hexahydrate [$NiCl_2 \cdot 6H_2O$], cobalt chloride hexahydrate [$CoCl_2 \cdot 6H_2O$], potassium perchlorate [$KClO_4$], and magnesium perchlorate [$Mg(ClO_4)_2$]. We also tested the sensitivity to As(III) using sodium (meta)arsenite [AsO_2Na]. All reagents were purchased from Sigma-Aldrich and dissolved in deionized water (18.2 MΩ*cm).

2.2. Ag Nanoclusters Synthesis

Silver nanoclusters were synthesized using a slightly modified procedure described in detail in a previous work [60]. Briefly, 2.5 mL of a water solution of $AgNO_3$ (50 mM) were mixed with a PMAA solution (5.6 mM) at room temperature under vigorous stirring. The pH value was adjusted to 4 by adding HNO_3 in order to have the right structural conformation of the polymer chains, avoiding the aggregation of AgNCs and to have the highest efficiency of fluorescence. As a final step, the mixture was exposed to a UV lamp (300 W, Oriel Instruments, Newport, RI, USA) for 6 min to promote the reduction reaction of silver ions to silver metal. Nitrogen gas was fluxed on the solution surface during all the UV exposition to hamper the oxidation of the growing AgNCs. The AgNCs-PMAA obtained were centrifuged to remove large nanoparticles and aggregates. The supernatant solution was collected and kept in the fridge before use.

2.3. Hybrid Hydrogel Matrix Synthesis

Photopolymerizable hydrogel matrix was synthesized using 5 mL of PEGDA$_{700}$, 4 mL of H_2O at pH = 4, 1 mL of AgNCs-PMAA, and 600 µL of Irgacure 819 (25 mg/mL in ethanol). All the components were mixed for 24 h in the dark. A total of 1.5 mL of the final mixture were inserted in a 4-faces plastic cuvette and exposed for 2 min under a low power UV table-lamp (λ = 366 nm, Minuvis, Desaga, Wiesloch, Germany). During the photopolymerization process, the energy was transferred to the photoinitiator molecules, breaking them in the form of radicals, which opened the double terminal bonds of the PEGDA chains. Finally, polymeric chains joined together, forming a solid network. The AgNCs-PMAA were trapped in the tri-dimensional network of the polymerized PEGDA with a very good homogeneity and the device was ready to be used in the Pb(II) detection measurements. In order to evaluate the effect on the sensitivity of the system, the concentration of AgNCs-PMAA in the matrix was changed, adding different volumes of bare AgNCs-PMAA solution to the matrix precursors. The volumes of 0.75 mL, 1 mL, 2 mL, 3 mL, and 5 mL were investigated. The Table S1 of Supplementary Materials provides the contents for each compound employed for the synthesis of the hybrid hydrogel.

2.4. Experimental Apparatuses and Sensing Measurement Protocol

The UV-Vis (range 200–700 nm) absorption spectra of the matrix compounds were collected using a Perkin-Elmer Lambda 19 spectrophotometer. The photoluminescence characterization was accomplished using a LED source (λ = 340 nm, M340L4, Thorlabs, Newton, MA, USA) as excitation, a 25 cm monochromator (Model 1231, Instruments SA Inc., Edison, NJ, USA), and a CCD (S7011-1007, HAMAMATSU, Hamamatsu city, Japan) as detector. The experiments were carried out in triplicate and for each sample, four emission spectra were recorded, one for each face of the cuvette. The fluorescence measurements of the different sides of the cuvette are reported in the Figure S2 of the Supplementary Materials, showing a very good reproducibility and a good homogeneity of the dispersion of the NCs in the solid matrix. For the sensing measurements, a long pass filter of 550 nm (FGL550, Thorlabs) was employed to cut the fluorescence band related to the solid matrix while maintaining the AgNCs-PMAA emission. The power of the LED was measured before and after each acquisition to guarantee the same light intensity for each sample. For the sensing protocol, one solid sample was taken as reference, while another was kept in contact with Pb(II) contaminated water (with a specific lead concentration) and subsequently the fluorescence was recorded. A volume of 1 mL of polluted water was inserted in the cuvette over the hydrogel matrix; in the case of the reference, simple

deionized water was employed. The sensing protocol was repeated for each AgNCs-PMAA concentration. The kinetics of interaction was followed recording the emission spectra of the hybrid hydrogel sensor polluted with 50 μM of Pb(II) for 25 h. The equilibrium value was reached after 18 h as reported in the Figure S3. After each measurements the sample was stored at T = 4 °C. Sensing tests were performed after 18 h of interaction. In addition, to evaluate the time stability of the matrix with AgNCs-PMAA and the reproducibility of the data, the fluorescence was studied over 5 days, showing that the PL intensity during this period is highly stable as reported in the Figure S4. The interaction kinetics represent a point of weakness due to the long time to reach the equilibrium, but this drawback could be easily overcome by photolithography techniques since the photopolymerizable material can be easily microstructured, increasing the surface interaction between AgNCs-PMAA and Pb(II) ions and decreasing the time kinetics.

The size and shape of the AgNCs-PMAA have been investigated by HRTEM. An image corrected FEI Titan Themis 60–300 X-FEG has been used for these studies. A 4 k × 4 k pixels on a metal-oxide-semi-conductor (CMOS) camera has been applied to acquire the HRTEM images.

3. Results and Discussion

3.1. Optical and Morphological Characterizations

In Figure 1, the optical absorptions (black curves) and the photoluminescence emissions (red lines) of the single components used for the matrix synthesis are shown. The photoinitiator (Figure 1a) shows a very high absorption for wavelengths shorter than 450 nm for a concentration that was the same used in the synthesis of the hybrid hydrogel matrix (25 mg/mL) and an emission band centered at about 510 nm. The $PEGDA_{700}$ (Figure 1b) shows a weak absorption band at 305 nm and a double peak emission at 485 nm and 510 nm, respectively. The absorption and the PL emission of the AgNCs-PMAA are shown in Figure 1c; the shoulder at 300 nm in the absorption spectrum is due to the presence of NO_3^- residual ions from the synthesis [61]. The AgNCs-PMAA aqueous solution exhibits a fluorescence peak at 660 nm. In Figure 1d, the absorption of the solid hydrogel matrix of $PEGDA_{700}$ and AgNCs-PMAA and its emission are shown. The fluorescence band clearly shows the two contributions originating from the AgNCs-PMAA and the solid $PEGDA_{700}$ hydrogel matrix.
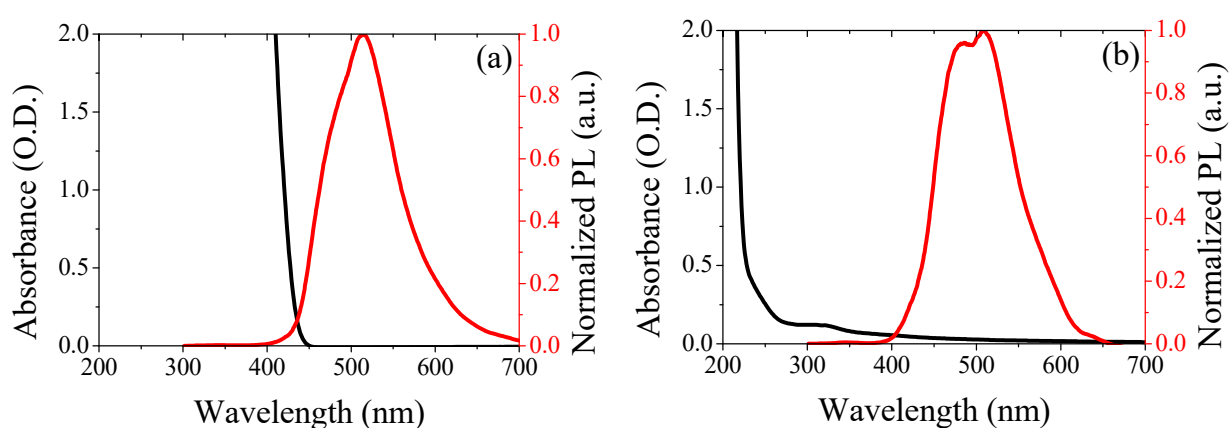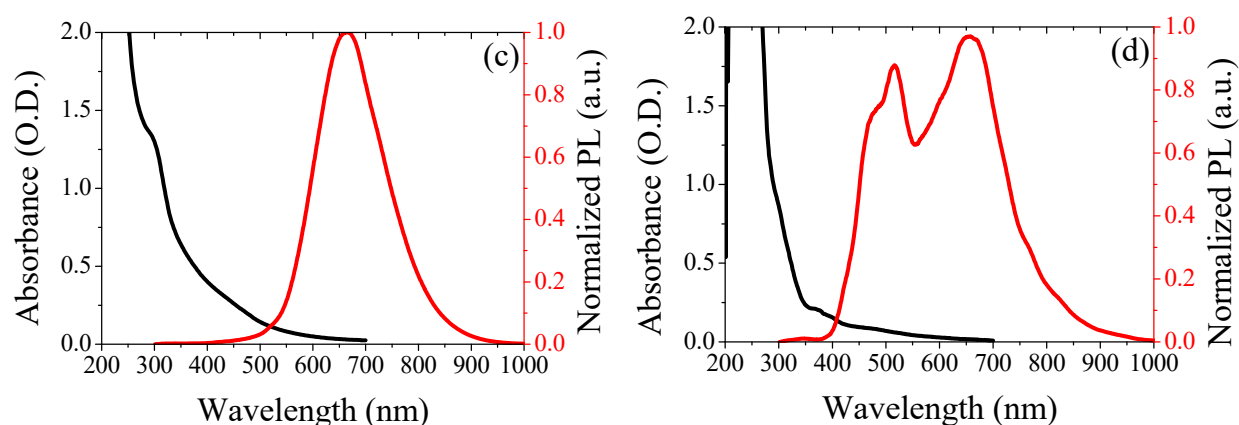

Figure 1. *Cont.*

Figure 1. UV-Vis absorption (black lines) and normalized PL emission (red lines) spectra of: (**a**) photoinitiator Irgacure 819, (**b**) PEGDA$_{700}$, (**c**) AgNCs-PMAA in aqueous solution, (**d**) solid hydrogel matrix of PEGDA$_{700}$ with AgNCs-PMAA.

The HRTEM images of the AgNCs-PMAA after the centrifugation process and before the embedding in the hybrid matrix is reported in Figure 2a,b, highlighting a mean size of 1.84 ± 0.60 nm. In Figure 2c, a picture of the solid optical device composed by the hydrogel matrix inside a plastic cuvette is reported.
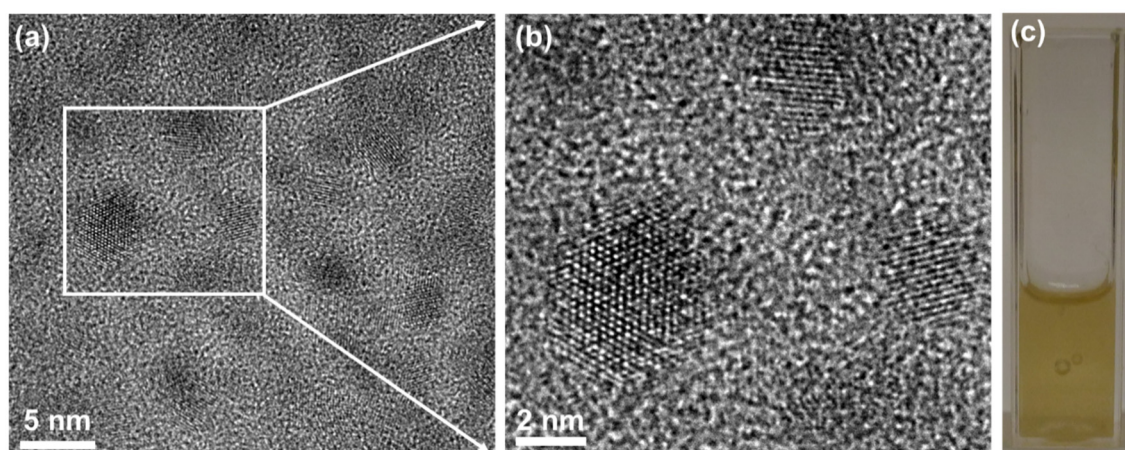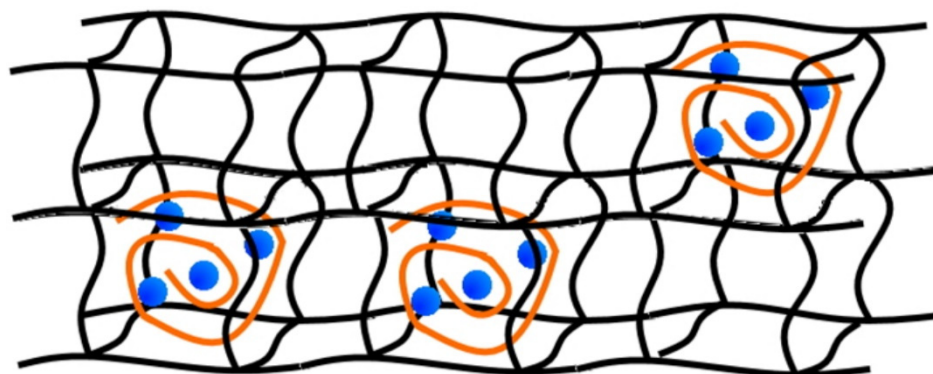

Figure 2. (**a**,**b**) HRTEM images of AgNCs-PMAA; (**c**) photograph of the AgNCs embedded in the PEGDA matrix inside the plastic cuvette.

In Scheme 1, a simple drawing of the structural arrangement of the AgNCs-PMAA in the PEGDA$_{700}$ matrix is reported. The black lines represent the crosslinked PEGDA chains while the orange-coiled lines are the PMAA polymer molecules and the blue spheres are the AgNCs. The crosslinking reaction traps the AgNCs-PMAA nanostructures within the PEGDA chain network, producing a stabilization of the fluorescent nanoclusters in a porous environment, which allows the diffusion of the Pb(II) contaminated drops of water added on the top of the solid matrix.

Scheme 1. Schematic representation of the structural arrangement of AgNCs-PMAA nanostructures trapped in the PEGDA$_{700}$ network.

3.2. Sensing Measurements

In a recent work [60], we tested the response of colloidal aqueous solution of AgNCs-PMAA in the presence of several heavy metal ions. Briefly, we have found an enhancement of the PL emission with respect to the reference solution for Zn(II), Cd(II), and Pb(II) with a fixed concentration of 50 μM, while for the same concentration of many other heavy metal ions, the fluorescence signal was the same as the reference one. The best response in terms of change of fluorescence intensity was found for Pb(II). The same experiment was carried out also in the case of the hybrid matrix containing AgNCs. The results are shown in Figure S5 of Supplementary Materials, highlighting that the selectivity was unchanged with respect to the trials in the liquid phase.

We focused our investigation to Pb(II) ions since they presented the highest optical response. The sensitivity is related to the AgNCs content; the study of different AgNCs-PMAA contents in the polymeric matrix has shown that the lower the amount of NCs, the higher the optical response in presence of Pb(II). Figure S6 shows the ratio F/F_0 as a function of Pb(II) concentration (0–100 μM) for different AgNCs densities, where F is the fluorescence intensity of the polluted sample and F_0 is the intensity of the reference sample. In this graph, the linear fittings for each case are also presented. The limit of detection (LOD, 3σ) for each sample was estimated and reported in the Table S7. The shape of the AgNCs emission for the lowest concentrated sample (0.75 mL) was too weak to be used for sensing tests. Therefore, the sample labelled with "1 mL" represents the best compromise among sensitivity and intensity of AgNCs emission. Figure 3a reports the PL spectra of the samples with different Pb(II) concentrations and the emission spectrum of bare AgNCs-PMAA colloidal solution as reference is included in the graph (dotted grey line). The PL intensity of the bare AgNCs-PMAA is arbitrary and not quantitatively comparable with the fluorescence of the hydrogel matrix. Figure 3b shows the F/F_0 ratio as a function of Pb(II) concentration. A linear behavior in the range 0–100 μM can be observed, while for higher contaminant concentrations, the F/F_0 ratio reaches a plateau where the value is almost constant. This is a clear indication that the centers responsible for the interaction with lead ions, namely the carboxyl groups of PMAA chains, are completely saturated by the polluting cations and an additional amount of lead ions does not produce a change in the fluorescence intensity of the nanoclusters. The limit of detection of doped hydrogel matrix was estimated. The value was 8 μM that compared to the AgNCs-PMAA colloidal solution was quite high. In that case, we found a low LOD of the order of 60 nM [60]. This behavior can be understood considering that fluorescence signal is a sum of two different fluorescence components. The first one was related to the fluorescence of the nanoclusters that increases with the increasing concentration of the lead ions. The second one was related to the PEGDA matrix itself. The sum of the two signals, producing an inseparable overlap, reduces the sensitivity of the system consistently. Nevertheless, the strategy to insert the sensitive elements in a solid matrix offers many advantages due to a greater stability in terms of handling, portability, and storage and the possibility of in situ

measurements. Moreover, the sensitivity of the solid system to Cd(II) and Zn(II) in addition to Pb(II) make this system potentially suitable to be used as a water filter for the removal of dangerous heavy metal ions. These preliminary results are very encouraging and open a new path towards solid-state optical sensors for Pb(II) ions based on fluorescent AgNCs.
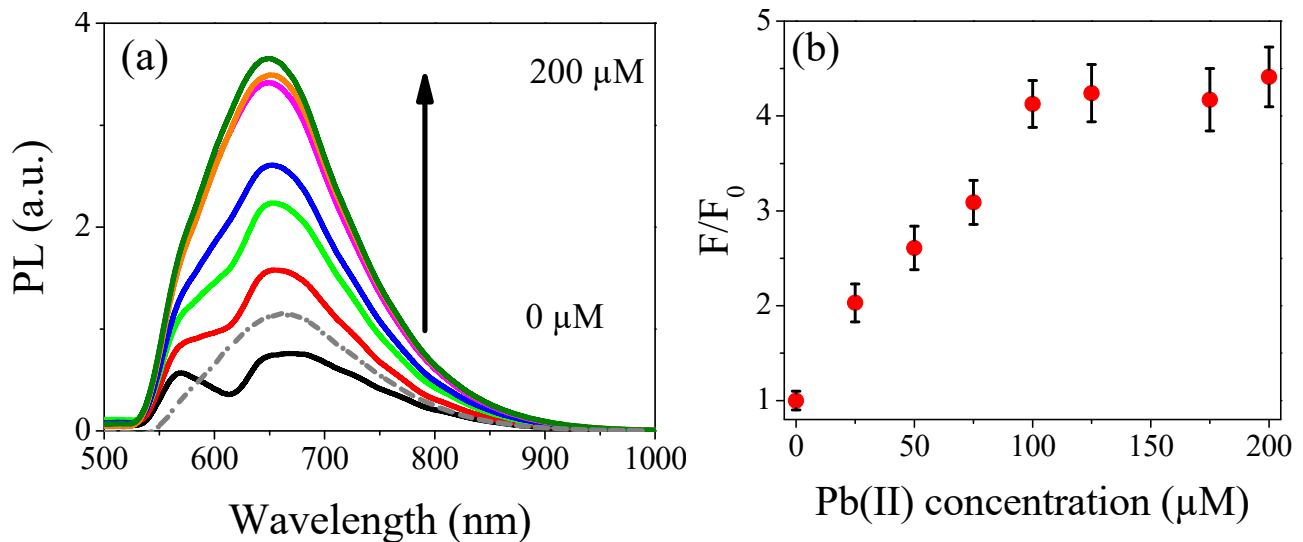

Figure 3. (**a**) PL spectra of the hydrogel matrix doped with AgNCs-PMAA as a function of Pb(II) concentration, the dotted grey line represents the emission of bare AgNCs-PMAA colloidal solution as reference; (**b**) the F/F_0 ratio as a function of Pb(II) concentration between 0–200 μM.

4. Conclusions

We synthesized highly monodispersed AgNCs-PMAA with a mean diameter of 1.84 nm using a simple photochemical approach. We embedded AgNCs-PMAA in a hydrogel matrix based on PEGDA. The photopolymerization of the matrix was easy and fast and the emission band of the NCs was still present. The hybrid hydrogel device preserves the sensitivity to Pb(II) ions thanks to the matrix porosity.

We measured a fluorescence intensity enhancement as a function of the Pb(II) ions present in water in contact with the solid matrix. This behavior can be used for lead detection in water with a good linearity up to 8 μM. Despite the high detection limit, with respect to the bare colloidal solution of AgNCs-PMAA, such a solid-state device is hugely more exploitable as an optical sensor than the liquid colloidal ones. These preliminary results are encouraging to fabricate an economic solid-state optical device for water monitoring that could be used directly for detection of lead ions on the field.

Conflicts of Interest: The authors declare no conflict of interest.

References

1. Mayer, K.M.; Hafner, J.H. Localized Surface Plasmon Resonance Sensors. *Chem. Rev.* **2011**, *111*, 3828–3857. [CrossRef] [PubMed]
2. Wei, L.; Lu, J.; Xu, H.; Patel, A.; Chen, Z.-S.; Chen, G. Silver nanoparticles: Synthesis, properties, and therapeutic applications. *Drug Discov. Today* **2015**, *20*, 595–601. [CrossRef] [PubMed]
3. Prosposito, P.; Burratti, L.; Venditti, I. Silver Nanoparticles as Colorimetric Sensors for Water Pollutants. *Chemosensors* **2020**, *8*, 26. [CrossRef]
4. Zannotti, M.; Vicomandi, V.; Rossi, A.; Minicucci, M.; Ferraro, S.; Petetta, L.; Giovannetti, R. Tuning of hydrogen peroxide etching during the synthesis of silver nanoparticles. An application of triangular nanoplates as plasmon sensors for Hg2+ in aqueous solution. *J. Mol. Liq.* **2020**, *309*, 113238. [CrossRef]
5. Coronado, E.A.; Encina, E.R.; Stefani, F.D. Optical properties of metallic nanoparticles: Manipulating light, heat and forces at the nanoscale. *Nanoscale* **2011**, *3*, 4042. [CrossRef]
6. Díez, I.; Pusa, M.; Kulmala, S.; Jiang, H.; Walther, A.; Goldmann, A.S.; Müller, A.H.E.; Ikkala, O.; Ras, R.H.A. Color Tunability and Electrochemiluminescence of Silver Nanoclusters. *Angew. Chemie Int. Ed.* **2009**, *48*, 2122–2125. [CrossRef] [PubMed]
7. Jin, R. Quantum sized, thiolate-protected gold nanoclusters. *Nanoscale* **2010**, *2*, 343–362. [CrossRef] [PubMed]
8. Lünskens, T.; Heister, P.; Thämer, M.; Walenta, C.A.; Kartouzian, A.; Heiz, U. Plasmons in supported size-selected silver nanoclusters. *Phys. Chem. Chem. Phys.* **2015**, *17*, 17541–17544. [CrossRef] [PubMed]
9. Aikens, C.M. Electronic and Geometric Structure, Optical Properties, and Excited State Behavior in Atomically Precise Thiolate-Stabilized Noble Metal Nanoclusters. *Acc. Chem. Res.* **2018**, *51*, 3065–3073. [CrossRef]
10. Chakraborty, I.; Pradeep, T. Atomically Precise Clusters of Noble Metals: Emerging Link between Atoms and Nanoparticles. *Chem. Rev.* **2017**, *117*, 8208–8271. [CrossRef]
11. Aikens, C.M. Origin of Discrete Optical Absorption Spectra of M 25 (SH) 18 − Nanoparticles (M = Au, Ag). *J. Phys. Chem. C* **2008**, *112*, 19797–19800. [CrossRef]
12. Yau, S.H.; Ashenfelter, B.A.; Desireddy, A.; Ashwell, A.P.; Varnavski, O.; Schatz, G.C.; Bigioni, T.P.; Goodson, T. Optical Properties and Structural Relationships of the Silver Nanoclusters Ag 32 (SG) 19 and Ag 15 (SG) 11. *J. Phys. Chem. C* **2017**, *121*, 1349–1361. [CrossRef]
13. Bolli, E.; Mezzi, A.; Burratti, L.; Prosposito, P.; Casciardi, S.; Kaciulis, S. X-ray and UV photoelectron spectroscopy of Ag nanoclusters. *Surf. Interface Anal.* **2020**. [CrossRef]
14. Lu, Y.; Wei, W.; Chen, W. Copper nanoclusters: Synthesis, characterization and properties. *Chinese Sci. Bull.* **2012**, *57*, 41–47. [CrossRef]
15. Muhammed, M.A.H.; Aldeek, F.; Palui, G.; Trapiella-Alfonso, L.; Mattoussi, H. Growth of in situ functionalized luminescent silver nanoclusters by direct reduction and size focusing. *ACS Nano* **2012**, *6*, 8950–8961. [CrossRef] [PubMed]
16. Burratti, L.; Bolli, E.; Casalboni, M.; de Matteis, F.; Mochi, F.; Francini, R.; Casciardi, S.; Prosposito, P. Synthesis of Fluorescent Ag Nanoclusters for Sensing and Imaging Applications. *Mater. Sci. Forum* **2018**, *941*, 2243–2248. [CrossRef]
17. Maretti, L.; Billone, P.S.; Liu, Y.; Scaiano, J.C. Facile Photochemical Synthesis and Characterization of Highly Fluorescent Silver Nanoparticles. *J. Am. Chem. Soc.* **2009**, *131*, 13972–13980. [CrossRef] [PubMed]
18. Liu, C.; Ding, Y.; Li, Q.; Lin, Y. Photochemical synthesis of glutathione-stabilized silver nanoclusters for fluorometric determination of hydrogen peroxide. *Microchim. Acta* **2017**, *184*, 2497–2503. [CrossRef]
19. Xu, H.; Suslick, K.S. Sonochemical Synthesis of Highly Fluorescent Ag Nanoclusters. *ACS Nano* **2010**, *4*, 3209–3214. [CrossRef]
20. Zhou, T.; Rong, M.; Cai, Z.; Yang, C.J.; Chen, X. Sonochemical synthesis of highly fluorescent glutathione-stabilized Ag nanoclusters and S2− sensing. *Nanoscale* **2012**, *4*, 4103. [CrossRef]
21. Wang, C.; Wang, Y.; Xu, L.; Zhang, D.; Liu, M.; Li, X.; Sun, H.; Lin, Q.; Yang, B. Facile aqueous-phase synthesis of biocompatible and fluorescent Ag2S nanoclusters for bioimaging: Tunable photoluminescence from red to near infrared. *Small* **2012**, *8*, 3137–3142. [CrossRef] [PubMed]
22. Le Guevel, X. Recent advances on the synthesis of metal quantum nanoclusters and their application for bioimaging. *IEEE J. Sel. Top. Quantum Electron.* **2014**, *20*. [CrossRef]
23. Yang, L.; Wang, H.; Li, D.; Li, L.; Lou, X.; Liu, H. Self-Nucleation and Self-Assembly of Highly Fluorescent Au 5 Nanoclusters for Bioimaging. *Chem. Mater.* **2018**, *30*, 5507–5515. [CrossRef]
24. Sarparast, M.; Noori, A.; Ilkhani, H.; Bathaie, S.Z.; El-Kady, M.F.; Wang, L.J.; Pham, H.; Marsh, K.L.; Kaner, R.B.; Mousavi, M.F. Cadmium nanoclusters in a protein matrix: Synthesis, characterization, and application in targeted drug delivery and cellular imaging. *Nano Res.* **2016**, *9*, 3229–3246. [CrossRef]
25. Bhattacharyya, K.; Mukherjee, S. Fluorescent Metal Nano-Clusters as Next Generation Fluorescent Probes for Cell Imaging and Drug Delivery. *Bull. Chem. Soc. Jpn.* **2018**, *91*, 447–454. [CrossRef]
26. Su, F.; Jia, Q.; Li, Z.; Wang, M.; He, L.; Peng, D.; Song, Y.; Zhang, Z.; Fang, S. Aptamer-templated silver nanoclusters embedded in zirconium metal–organic framework for targeted antitumor drug delivery. *Microporous Mesoporous Mater.* **2019**, *275*, 152–162. [CrossRef]
27. Abroshan, H.; Li, G.; Lin, J.; Kim, H.J.; Jin, R. Molecular mechanism for the activation of Au25(SCH2CH2Ph)18 nanoclusters by imidazolium-based ionic liquids for catalysis. *J. Catal.* **2016**, *337*, 72–79. [CrossRef]

28. Deraedt, C.; Melaet, G.; Ralston, W.T.; Ye, R.; Somorjai, G.A. Platinum and Other Transition Metal Nanoclusters (Pd, Rh) Stabilized by PAMAM Dendrimer as Excellent Heterogeneous Catalysts: Application to the Methylcyclopentane (MCP) Hydrogenative Isomerization. *Nano Lett.* **2017**, *17*, 1853–1862. [CrossRef]

29. Du, X.; Jin, R. Atomically Precise Metal Nanoclusters for Catalysis. *ACS Nano* **2019**, *13*, 7383–7387. [CrossRef]

30. Lan, J.; Zhang, P.; Wang, T.T.; Chang, Y.; Lie, S.Q.; Wu, Z.L.; De Liu, Z.; Li, Y.F.; Huang, C.Z. One-pot hydrothermal synthesis of orange fluorescent silver nanoclusters as a general probe for sulfides. *Analyst* **2014**, *139*, 3441–3445. [CrossRef]

31. Pan, S.; Liu, W.; Tang, J.; Yang, Y.; Feng, H.; Qian, Z.; Zhou, J. Hydrophobicity-guided self-assembled particles of silver nanoclusters with aggregation-induced emission and their use in sensing and bioimaging. *J. Mater. Chem. B* **2018**, *6*, 3927–3933. [CrossRef] [PubMed]

32. Burratti, L.; Ciotta, E.; De Matteis, F.; Prosposito, P. Metal Nanostructures for Environmental Pollutant Detection Based on Fluorescence. *Nanomaterials* **2021**, *11*, 276. [CrossRef] [PubMed]

33. Tsade, H. Atomic Absorption Spectroscopic Determination of Heavy Metal Concentrations in Kulufo River, Arbaminch, Gamo Gofa, Ethiopia. *J. Environ. Anal. Chem.* **2016**, *3*, 1–3. [CrossRef]

34. Hieftje, G.M. Atomic Emission Spectroscopy—It Lasts and Lasts and Lasts. *J. Chem. Educ.* **2000**, *77*, 577. [CrossRef]

35. Zhou, Q.; Lei, M.; Liu, Y.; Wu, Y.; Yuan, Y. Simultaneous determination of cadmium, lead and mercury ions at trace level by magnetic solid phase extraction with Fe@Ag@Dimercaptobenzene coupled to high performance liquid chromatography. *Talanta* **2017**, *175*, 194–199. [CrossRef]

36. Aydin, F.A.; Soylak, M. Separation, preconcentration and inductively coupled plasma-mass spectrometric (ICP-MS) determination of thorium(IV), titanium(IV), iron(III), lead(II) and chromium(III) on 2-nitroso-1-naphthol impregnated MCI GEL CHP20P resin. *J. Hazard. Mater.* **2010**, *173*, 669–674. [CrossRef] [PubMed]

37. Farrukh, M.A. *Atomic Absorption Spectroscopy*, 1st ed.; Akhyar Farrukh, M., Ed.; InTech: London, UK, 2012; ISBN 978-953-307-817-5.

38. Nain, A.; Tseng, Y.-T.; Lin, Y.-S.; Wei, S.-C.; Mandal, R.P.; Unnikrishnan, B.; Huang, C.-C.; Tseng, F.-G.; Chang, H.-T. Tuning the photoluminescence of metal nanoclusters for selective detection of multiple heavy metal ions. *Sens. Actuators B Chem.* **2020**, 128539. [CrossRef]

39. Xiao, N.; Dong, J.X.; Liu, S.G.; Li, N.; Fan, Y.Z.; Ju, Y.J.; Li, N.B.; Luo, H.Q. Multifunctional fluorescent sensors for independent detection of multiple metal ions based on Ag nanoclusters. *Sens. Actuators B Chem.* **2018**, *264*, 184–192. [CrossRef]

40. George, A.; Gopalakrishnan, H.; Mandal, S. Surfactant free platinum nanocluster as fluorescent probe for the selective detection of Fe (III) ions in aqueous medium. *Sens. Actuators B Chem.* **2017**, *243*, 332–337. [CrossRef]

41. Xu, J.; Han, B. Synthesis of Protein-Directed Orange/Red-Emitting Copper Nanoclusters via Hydroxylamine Hydrochloride Reduction Approach and Their Applications on Hg2+ Sensing. *Nano* **2016**, *11*, 1650108. [CrossRef]

42. Zhang, J.R.; Zeng, A.L.; Luo, H.Q.; Li, N.B. Fluorescent silver nanoclusters for ultrasensitive determination of chromium(VI) in aqueous solution. *J. Hazard. Mater.* **2016**, *304*, 66–72. [CrossRef] [PubMed]

43. Che, Y.; Zinchenko, A.; Murata, S. Control of a catalytic activity of gold nanoparticles embedded in DNA hydrogel by swelling/shrinking the hydrogel's matrix. *J. Colloid Interface Sci.* **2015**, *445*, 364–370. [CrossRef] [PubMed]

44. Juby, K.A.; Dwivedi, C.; Kumar, M.; Kota, S.; Misra, H.S.; Bajaj, P.N. Silver nanoparticle-loaded PVA/gum acacia hydrogel: Synthesis, characterization and antibacterial study. *Carbohydr. Polym.* **2012**, *89*, 906–913. [CrossRef] [PubMed]

45. Al-Enizi, A.M.; Ahamad, T.; Al-hajji, A.B.; Ahmed, J.; Chaudhary, A.A.; Alshehri, S.M. Cellulose gum and copper nanoparticles based hydrogel as antimicrobial agents against urinary tract infection (UTI) pathogens. *Int. J. Biol. Macromol.* **2018**, *109*, 803–809. [CrossRef]

46. Qindeel, M.; Ahmed, N.; Sabir, F.; Khan, S.; Ur-Rehman, A. Development of novel pH-sensitive nanoparticles loaded hydrogel for transdermal drug delivery. *Drug Dev. Ind. Pharm.* **2019**, *45*, 629–641. [CrossRef] [PubMed]

47. Gulsonbi, M.; Parthasarathy, S.; Bharat Raj, K.; Jaisankar, V. Green synthesis, characterization and drug delivery applications of a novel silver/carboxymethylcellulose—poly(acrylamide) hydrogel nanocomposite. *Ecotoxicol. Environ. Saf.* **2016**, *134*, 421–426. [CrossRef] [PubMed]

48. Lim, J.Y.C.; Goh, S.S.; Loh, X.J. Bottom-Up Engineering of Responsive Hydrogel Materials for Molecular Detection and Biosensing. *ACS Mater. Lett.* **2020**, *2*, 918–950. [CrossRef]

49. MacLean, J.L.; Morishita, K.; Liu, J. DNA stabilized silver nanoclusters for ratiometric and visual detection of Hg2+ and its immobilization in hydrogels. *Biosens. Bioelectron.* **2013**, *48*, 82–86. [CrossRef] [PubMed]

50. Yuan, Z.; Cai, N.; Du, Y.; He, Y.; Yeung, E.S. Sensitive and Selective Detection of Copper Ions with Highly Stable Polyethyleneimine-Protected Silver Nanoclusters. *Anal. Chem.* **2014**, *86*, 419–426. [CrossRef]

51. Pourreza, N.; Ghomi, M. In situ synthesized and embedded silver nanoclusters into poly vinyl alcohol-borax hydrogel as a novel dual mode "on and off" fluorescence sensor for Fe (III) and thiosulfate. *Talanta* **2018**, *179*, 92–99. [CrossRef]

52. Shen, X.; Yang, X.; Su, C.; Yang, J.; Zhang, L.; Liu, B.; Gao, S.; Gai, F.; Shao, Z.; Gao, G. Thermo-responsive photoluminescent silver clusters/hydrogel nanocomposites for highly sensitive and selective detection of Cr(VI). *J. Mater. Chem. C* **2018**, *6*, 2088–2094. [CrossRef]

53. Pinelli, F.; Magagnin, L.; Rossi, F. Progress in hydrogels for sensing applications: A review. *Mater. Today Chem.* **2020**, *17*, 100317. [CrossRef]

54. Castro, D.; Ingram, P.; Kodzius, R.; Conchouso, D.; Yoon, E.; Foulds, I.G. Characterization of solid UV cross-linked PEGDA for biological applications. In Proceedings of the 2013 IEEE 26th International Conference on Micro Electro Mechanical Systems (MEMS), Taipei, Taiwan, 20–24 January 2013; pp. 457–460.

55. Yang, W.; Yu, H.; Liang, W.; Wang, Y.; Liu, L. Rapid Fabrication of Hydrogel Microstructures Using UV-Induced Projection Printing. *Micromachines* **2015**, *6*, 1903–1913. [CrossRef]

56. Sannino, A.; Netti, P.A.; Madaghiele, M.; Coccoli, V.; Luciani, A.; Maffezzoli, A.; Nicolais, L. Synthesis and characterization of macroporous poly(ethylene glycol)-based hydrogels for tissue engineering application. *J. Biomed. Mater. Res. Part A* **2006**, *79A*, 229–236. [CrossRef] [PubMed]

57. Caldorera-Moore, M.; Kang, M.K.; Moore, Z.; Singh, V.; Sreenivasan, S.V.; Shi, L.; Huang, R.; Roy, K. Swelling behavior of nanoscale, shape- and size-specific, hydrogel particles fabricated using imprint lithography. *Soft Matter* **2011**, *7*, 2879. [CrossRef]

58. Shang, L.; Dong, S. Sensitive detection of cysteine based on fluorescent silver clusters. *Biosens. Bioelectron.* **2009**, *24*, 1569–1573. [CrossRef] [PubMed]

59. Shen, Z.; Duan, H.; Frey, H. Water-soluble fluorescent ag nanoclusters obtained from multiarm star poly(acrylic acid) as "molecular hydrogel" templates. *Adv. Mater.* **2007**, *19*, 349–352. [CrossRef]

60. Burratti, L.; Ciotta, E.; Bolli, E.; Kaciulis, S.; Casalboni, M.; De Matteis, F.; Garzón-Manjón, A.; Scheu, C.; Pizzoferrato, R.; Prosposito, P. Fluorescence enhancement induced by the interaction of silver nanoclusters with lead ions in water. *Colloids Surf. A Physicochem. Eng. Asp.* **2019**, *579*, 123634. [CrossRef]

61. Gvozdi, V.; Butorac, V.; Simeon, V. Association of Nitrate Ion with Metal Cations in Aqueous Solution: A UV-Vis Spectrometric and Factor-Analytical Study. *Croat. Chem. Acta* **2009**, *82*, 553–559.